Journal of Molecular Structure 1215 (2020) 128247

Contents lists available at ScienceDirect

Journal of Molecular Structure

journal homepage: http://www.elsevier.com/locate/molstruc

Synthesis, characterization and computational studies of 4-[(Pyridine-3-carbonyl)-hydrazonomethyl]-benzoic acid

Füreya Elif Öztürkkan Özbek [a, *], Güventürk Uğurlu [b, **], Erbay Kalay [c], Hacali Necefoğlu [d, e]

[a] Kafkas University, Department of Chemical Engineering, 36100, Kars, Turkey
[b] Kafkas University, Department of Physics, 36100, Kars, Turkey
[c] Kafkas University, Kars Vocational College, 36100, Kars, Turkey
[d] Kafkas University, Department of Chemistry, 36100, Kars, Turkey
[e] Baku State University, International Scientific Research Centre, 1148, Baku, Azerbaija

ARTICLE INFO

Article history:
Received 24 January 2020
Received in revised form
8 April 2020
Accepted 11 April 2020
Available online xxx

Keywords:
Aroylhydrazones
Nicotinohydrazides
Molecular geometry
Hyperpolarizability
NLO

ABSTRACT

A new hydrazone derivative compound, 4-[(Pyridine-3-carbonyl)-hydrazonomethyl]-benzoic acid, $C_{15}H_{11}N_3O$, was obtained and characterized by ^{1}H NMR, ^{13}C NMR and UV–Vis, FT-IR and FT-Raman spectroscopy techniques. Molecular geometry, vibrational wavenumbers, frontier molecular orbital and non-linear optical (NLO) property of the title compound were calculated using ab initio Hartree-Fock (HF) and Density Functional Theory (DFT), employing B3LYP functional at 6–311++G (d,p) basis set. ^{1}H and ^{13}C NMR chemical shifts were calculated by using the gauge in dependent atomic orbital (GIAO) method at the HF and B3LYP methods with different basis sets. In addition, the highest occupied molecular orbital (HOMO) and the lowest unoccupied molecular orbital (LUMO) were obtained from DFT LSDA methods with 6–311++G (d,p) basis set. The NLO behaviour of the title compound has been studied by determining the electric dipole moment (μ) and hyperpolarizability (β) using both B3LYP/6–311++G (d,p) and HF/6–311++G (d,p) methods. The energy gaps s($\Delta E_{gap} = E_{LUMO} - E_{HOMO}$) of title molecule were calculated at 4.15, 2.77 and 9.81 eV with DFT-B3LYP/6–311++ G (d,p), DFT-LSDA/6–311++ G (d,p) and HF/6–311++ G (d,p) level of theory, respectively. The calculated experimentally energy gap was found as 2.827 eV.

© 2020 Elsevier B.V. All rights reserved.

1. Introduction

Nicotinic acid derivatives are very important in biological activities such as anti-parkinsonian, anti-tubercular, antihelmintic, antifungicidal, antitumor and anti-bacterial activities [1–3]. Nicotinic acid hydrazides give the significant effect on toxicity to the insects [4]. The chemistry aroylhydrazones derived from nicotinic acid hydrazide have been intensively studied due to their biological and physico-chemical properties and applications. Nicotinohydrazides posses antimycobacterial, antiviral, antimicrobial [5], antituberculosis [6], anticonvulsant [7], anti-inflammatory and analgestic [8,9], insecticidal [4] activities. Recent studies have shown that nicotinohydrazides could be potentially used as analytical reagents for spectrophotometric determination of V(V) [10], Cu(II) and spectrofluorimetric determination of Al(III) [11,12]. Some aromatic hydrazones derived from nicotinic acid hydrazide are potential fluorimetric pH sensors [13]. The efficiency of 1-(4-propylbenzylidene)nicotinohydrazide has been studied as corrosion inhibitor of mild steel [14].

Structures of aroylhydrazones derived from nicotinic acid hydrazide have been investigated in solid state, in solution and gas phase by FT-IR, NMR, UV–Vis, ATR and Raman spectroscopy, ESI-MS and MS/MS analysis techniques [15–17]. The protonation constants and hydrolytic stability of nicotinohydrazides have been studied by using of spectrophotometric, HPLC and MS measurements [18]. The dipole moments, polarizability and first order hyperpolarizability of N'-(2-metyl-3-phenylallylidene)nicotinohydrazide and its isonicotinohydrazide analog have been computed and calculated. The first order hyperpolarizabilities have revealed that both hydrazides behave as interesting NLO materials [19].

The coordination abilities of transition metal complexes of aroylhydrazones have made them attractive as ligands for the synthesis of new coordination compounds dioxomolybdenum (VI)

* Corresponding author.
** Corresponding author.
E-mail addresses: elif@kafkas.edu.tr (F. Elif Öztürkkan Özbek), gugurlu@kafkas.edu.tr (G. Uğurlu).

https://doi.org/10.1016/j.molstruc.2020.128247
0022-2860/© 2020 Elsevier B.V. All rights reserved.

complexes 2-hydroxybenzaldehyde nicotinoylhydrazone and vanadium(V) complex of N′-(3,5-dibromo-2-hydroxybenzylidene) nicotinohydrazide are an effective catalysis for oxydation of alifatic and aromatic olefines [20–22]. The cytotoxicity against human lung cancer, human gastric cancer and human esophageal cancer cell lines of (E)-N'-(1-(pyridin-2-yl)ethylidene)nicotinohydrazide nicotinohydrazide and its Mn(II), Co(II), Cu(II), Cd(II) complexes have been investigated [23]. The antitubercular activities of 2,6-dihydroxybenzaldehyde nicotinoylhydrazone, 5-chloro-2-hydroxybenzaldehyde nicotinoylhydrazone and some transition metal complexes of them have been evaluated against H37Rv strain of *Mycobacterium tuberculosis*, in vitro [24,25]. Lead nicotinohydrazides have interesting structures due to the presence of tetrel bonds [26,27].

Despite the fact that the crystalline structures of aroylhydrazones derived from nicotinic acid hydrazide have been investigated using single crystal X-ray diffraction in recent years [15,25,28–33], there are a few theoretical studies of them [34,35]. In addition, to the best of our knowledge, among the substances so far studied aroylhydrazones derived from nicotinic acid hydrazide the title compound is absent. In order to eliminate this deficiency, we synthesized title compound and characterized by Fourier-Transform Infrared (FT-IR) and Fourier-Transform Raman (FT-Raman) and ^{1}H, ^{13}C NMR and UV–Vis spectroscopy techniques. A series of Hartree-Fock (HF) and Density Functional Theory (DFT) calculations on the title compound were reported in this paper. The optimized structure of 4-[(Pyridine-3-carbonyl)-hydrazonomethyl]-benzoic acid molecule with atomic number scheme in B3LYP/6–311++G (d.p) level was given in Fig. 1.

2. Materials and methods

All starting materials and solvents were purchased from commercial sources and used without further purification. Crystal water determination and thermal analyses were performed by the Shimadzu DTG-60H system, in a dynamic nitrogen atmosphere (100 mL/min), at a heating rate of 10 °C/min, in platinum sample vessels with reference to α-Al_2O_3. Melting point was determined in open glass capillary using a Stuart melting point SMP30 apparatus. Infrared and Raman spectra of the compound were recorded in the range of 4000–400 cm^{-1} on an ALPHA-P Bruker FT-IR spectrometer and Thermo Scientific/Nicolet IS50 Raman spectrometer from solid sample, respectively. UV–Vis spectra were recorded on a PerkinElmer's LAMBDA 25 Spectrophotometer and Schimadzu 3600/UV-VIS-NIR Spectrophotometer in DMSO. NMR Spectra were recorded at 400 MHz (^{1}H) and 101 MHz (^{13}C) at 298 K using tetramethylsilane (0 ppm) as the internal reference. NMR spectroscopic data were recorded in DMSO-d_6 using as internal standards the residual non-deuteriated signal for ^{1}H NMR and the deuteriated solvent signal for ^{13}C NMR spectroscopy. Chemical shifts (δ) are given in ppm, and coupling constants (J) are given in Hertz. The following abbreviations are used for multiplicities: s = singlet, d = doublet, t = triplet, q = quartet, dd = doublet of doublets and m = multiplet.

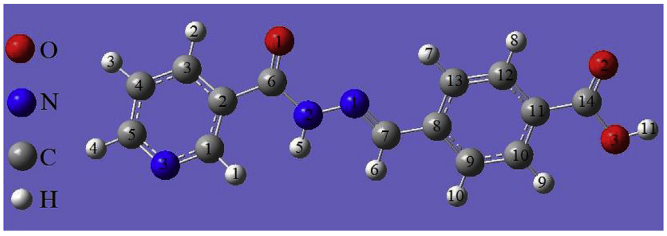

Fig. 1. The optimized structure of the molecule and and its numbering scheme.

Pyridine-3-carbohydrazide was prepared according to the literature [6].

2.1. Synthesis of the pyridine-3-carbohydrazide

In a 100 mL round-bottom flask, methylnicotinate **1** (2.74 g, 20 mmol) was dissolved in methanol (99%, 50 mL), and hydrazine hydrate (0.97 mL, 20 mmol) was added. The reaction mixture was heated under reflux conditions for 2 h. Progress of the reaction was monitored by TLC. After completion of the reaction, the mixture was cooled to room temperature. The solvent was concentrated in vacuo. The residue was redissolved in ethyl acetate (50 mL). Subsequently, the mixture was extracted with water (2 × 30 mL). The combined organic layers were dried over anhydrous Na_2SO_4, filtered and removed under reduced pressure. The hydrazide **2** was used in the following reaction without further purification (white solid, yield: 79%, m. p: 161–163 °C).

2.2. Synthesis of the 4-[(Pyridine-3-carbonyl)-hydrazonomethyl]-benzoic acid

In a 100 mL round-bottom flask, pyridine-3-carbohydrazide **2** (2.00 g, 14.6 mmol) and 4-formylbenzoic acid **3** (2.19 g, 14.6 mmol) were dissolved in methanol (60 mL) at room temperature. Then a few drops of glacial acetic acid as a catalyst were added. This mixture was heated under reflux for 5 h. The desired compound was monitored by TLC analysis. The mixture cooled to room temperature. Methanol was removed in vacuo and the precipitate obtained was suspended in a mixture of methanol-water (1:1, 3 × 10 mL), filtered off. After FT-IR spectra and thermal analysis results of 4-[(pyridine-3-carbonyl)-hydrazonomethyl]-benzoic acid monohydrate were evaluated, this compound was dried in a vacuum oven to afford the 4-[(pyridine-3-carbonyl)-hydrazonomethyl]-benzoic acid **4** (2.94 g, white solid, yield 75%, m. p: 317–319 °C). The reactions were given in above reaction scheme.

^{1}H NMR (400 MHz, DMSO-d_6, ppm) δ 13.11 (br s, 1H, OH), 12.18 (s, 1H, NH), 9.09 (s, 1H, CH=N), 8.79–8.78 (m, 1H), 8.51 (s, 1H), 8.28 (d, J = 7.8 Hz, 1H), 8.03 (d, J = 8.0 Hz, 2H, Ar–H), 7.87 (d, J = 8.1 Hz, 2H, Ar–H), 7.59 (dd, J = 7.5, 5.0 Hz, 1H); ^{13}C NMR (100 MHz, DMSO-d_6, ppm) δ 167.4 (Cq, C=O), 162.4 (Cq, C=O), 152.9 (CH), 149.1 (CH), 147.7 (CH), 138.6 (Cq), 136.0 (CH), 132.4 (Cq), 130.3 (CH), 129.5 (Cq), 127.7 (CH), 124.1 (CH); FT-IR (Solid Sample, cm^{-1}) 3482, 3432, 3214, 3072, 2358, 2343, 1666, 1605, 1560, 1508, 1473, 1409, 1363, 1333, 1317.

2.3. Computational details

All computational studies on the title molecule were performed by the aid of Gaussian 09 W program package and Gauss view 5.0 molecular visualization programs [36,37]. Initial geometries were optimized at ab-initio-HartreFock (HF) [38] and Density Functional Theory (DFT) with Becke's three parameter hybrid functional (B3) [39] and combined with gradient corrected correlation functional of Lee–Yang–Parr (LYP) [40,41] and employing 6–311++G (d,p) basis set [42,43] in the gas phase. In order to obtain the best stable structures, conformational analysis of the optimized molecule was performed as a function of dihedral angles ϕ1 (C3–C2–C6–N2), ϕ2 (N3–C7–C8–C13) and ϕ3 (C10–C11–C14–O2) which were varied between 0 and 360° in 10° steps with B3LYP/6-31G level of theory. The global energy minimum of each potential energy curves was referred to as zero. After optimization, vibrational frequencies, μ, α, β based on finite field approach, HOMO and LUMO of the title molecule in the ground states obtained B3LYP/6–311++G (d,p) and HF/6–311++G (d,p) level of theory were calculated in the same as level of theory. The ^{1}H and ^{13}C NMR chemical shifts were calculated

by GIAO approach by using B3LYP and HF methods with 6−311++G (d,p), 6-311 + G (2d,p) and 6−311++G (2d,p) basis sets both in the gas phase and in DMSO. Also, E_{HOMO} (the highest occupied molecular orbital energy) and E_{LUMO} (the lowest unoccupied molecular orbital energy) of title molecule were calculated at the DFT methods; local-spin density approximation LSDA with 6−311++G (d,p) basis sets.

3. Results and discussion

3.1. NMR spectra

Nuclear Magnetic Resonance Spectroscopy (NMR) is the useful technique for understanding the relationship between the electronic features and the structure of compounds. In this study, experimental ^{1}H and ^{13}C NMR spectra of the title compound were measured in DMSO-d_6. The obtained experimental data for ^{1}H and ^{13}C NMR spectra were used to determine the molecular structure and these data were compared with those obtained theoretically.

In the ^{1}H NMR spectra, the carboxylic acid O−H proton in title compound appeared as a singlet signal at 12.18 ppm. The N−H proton observed as a singlet signal at 9.09 ppm. The aromatic protons of the benzene and pyridine rings were observed among the 8.27−8.79 ppm and at 8.04−7.58 ppm in regions of spectrum, respectively. In ^{13}C NMR spectra, C=O carbon atom of carboxylic acid (C14) showed as very sharp signal at 167.4 ppm. The signals of aromatic carbons of pyridine ring were observed at 147.7 (C1), 130.3 (C2), 136.0 (C3), 124.1 (C4), 149.1 (C5) ppm. The singlet signal for imine carbon was seen at 152.9 ppm. The signals of aromatic carbons of benzene ring were observed at 138.6 (C8), 130.1 (C9), 129.5 (C10), 127.7 (C11), 132.4 (C12), 127.7 (C13) ppm. A singlet signal belonged to C=O carbon atom of carbonyl was showed at 162.4 ppm (Fig. 2).

The isotropic chemical shift analysis allows us to identify relative ionic species and to calculate reliable magnetic properties in nuclear magnetic resonance (NMR) spectroscopy which provide the accurate predictions of molecular geometries, [44−46]. For this purpose, the optimized molecular geometry of the titled compound was obtained by using B3LYP and HF methods with 6−31G (d) basis level in DMSO solvent. By considering the ^{1}H and ^{13}C NMR chemical shift values of the molecule were calculated at the same level by using Gauge-Independent Atomic Orbital method (Table 1). Theoretically and experimentally values were plotted according to δ exp = a. δ calc.+ b, Eq. a and b constants regression coefficients with a standard error values were found using the SigmaPlot program. The correlation graphics and linear correlation data of the titled compound were given Fig. 3.

Therefore the (R^2) values (DFT/HF) for ^{1}H NMR/^{13}C NMR chemical shifts have been found as 0.9714/0.6419, 0.9723/0.6293 and 0.9723/0.6311 for the title compound according to B3LYP/HF 6−311++G (d,p), B3LYP/HF 6-311 + G (2d,p) and B3LYP/HF 6−311++G (2d,p), respectively (Fig. 2). In our study, in the 1H NMR spectrum of corresponding compound, it was observed belong to H7 proton signal at 12.18 ppm because acidic show feature [47−49]. However, theoretically (DFT/HF) H7 proton has been observed as 10.74/10.12, 10.82/10.17 and 10.84/10.18 according to B3LYP/HF 6−311++G (d,p), B3LYP/HF 6-311 + G (2d,p) and B3LYP/HF 6−311++G (2d,p) methods, respectively (Fig. 2). It was observed that there was a correlation between the calculated and experimentally obtained values except for H7 proton. However, there was a higher than expected difference between the calculated values and the experimental values for H7 proton.

In Table 1, the biggest ^{13}C chemical shift value of the compound observed at 167.00 ppm for the C14 carbon atom double bounded to the oxygen in carbonyl group [48]. Theoretically, the calculated ppm values (DFT/HF) for C14 carbon atom were found as 171.8/167.3, 171.2/166.9 and 171.8/167.0 ppm according to B3LYP/HF 6−311++G (d,p), B3LYP/HF 6-311 + G (2d,p) and B3LYP/HF 6−311++G (2d,p), respectively. It was found that the results closest to the experimental value were B3LYP/6−311++G (d,p) when the experimental data were compared with theoretically calculated three different methods.

3.2. Vibrational analysis

The vibrational spectra of substituted benzene derivatives have been greatly investigated by various spectroscopic methods, since the single substitution can have a tendency to put greater changes in vibrational wavenumbers of benzene [50,51]. In other words, molecular system of benzene is greatly affected by the nature of substituents. The number of potentially active fundamentals of non-linear molecule which have N atoms is equal to (3N-6) apart from three translational and three rotational degrees of freedom. The title molecule contains 31 atoms and 87 normal vibration modes have C1 symmetry (Supplemental Table 1).

In the spectra of the title compound, it was observed a medium band at 3482 cm^{-1} due to ν(O−H). This absorption band was obtained among 3736 and 3613 cm^{-1} with help of HF and DFT/B3LYP methods at 6-31G (6−311++G (d,p) bases set calculations for FT-IR, respectively. The weak bands observed at 3400 and 3300 cm^{-1} in the FT-Raman spectrum are assigned to O−H stretching vibrations. This vibrations were computed among 3645 and 3656 cm^{-1} with help of HF and DFT/B3LYP methods at 6-31G (6−311++G (d,p) bases set calculations for FT-Raman spectra, respectively. The peaks displayed at a 3214 cm^{-1} (for FT-IR) and 3257 cm^{-1} (for FT-Raman), which is attributed to the N−H stretching vibration. The vibration frequency for N−H stretching was calculated to be 3219 cm^{-1} and 3378 cm^{-1} with help of HF and DFT for FT-Raman. The aromatic C−H stretching vibrations for pyridine and benzene rings were observed at 3072 cm^{-1} (for FT-IR) and 3057 cm^{-1} (for FT-Raman). The theoretically calculated value of C−H stretching vibrations were found to be between 3059 and 2907 cm^{-1} at HF and 3076-2889 cm^{-1} at DFT/B3LYP methods at 6−311++G (d,p) bases set for FT-IR spectra. In the FT-Raman spectra obtained from DFT and HF methods, these vibrations were seen as weak vibrations. The bands related to the carbonyl and carboxylic group C=O stretching vibrations were observed at 1666 cm^{-1} and 1605 cm^{-1} (for FT-IR spectra) and 1628 cm^{-1} and 1611 cm^{-1}. The C=O stretching vibrations (C6−O1) of carbonyl group were calculated to be 1754 cm^{-1} at B3LYP/6−311++G (d,p) and 1792 cm^{-1} at HF/6−311++G (d,p). The C=O stretching vibrations (C14−O2) of carboxylic group were found to be 1732 cm^{-1} B3LYP/6−311++G (d,p) and 1766 cm^{-1} HF/6−311++G (d,p) for FT-IR spectra. In FT-IR spectra of compound, the bands at 1605 and 1560 cm^{-1} were assigned to υ(C=N) and υ(N=N) respectively. These peaks were computed at 1643 and 1616 cm^{-1} group at B3LYP/6−311++G (d,p). The C7−N1 stretching vibration was calculated to be 1269 cm^{-1} at B3LYP/6−311++G (d,p) and 1215 cm^{-1} at HF/6−311++G (d,p) level of theory [52,53]. In FT-Raman spectra of compound, the bands at 1571 cm^{-1} and 1569 cm^{-1} are assigned to υ(C=N) and υ(N=N), respectively. Similar vibrations were observed in the FT-Raman spectra obtained with the help of HF and DFT methods.

The differences between the experimental and theoretical values of mentioned vibrations were based on from non-covalent interactions such as intermolecular and intramolecular hydrogen bonds (Fig. 4 a, c, d). Unlike mentioned peaks, in the FT-IR spectra of 4-[(pyridine-3-carbonyl)-hydrazonomethyl]-benzoic acid monohydrate, the O−H vibrations caused by the water molecule were observed 3600-3300 cm^{-1} in the region (Fig. 4-b). FT-Raman spectra were given in Fig. 5.

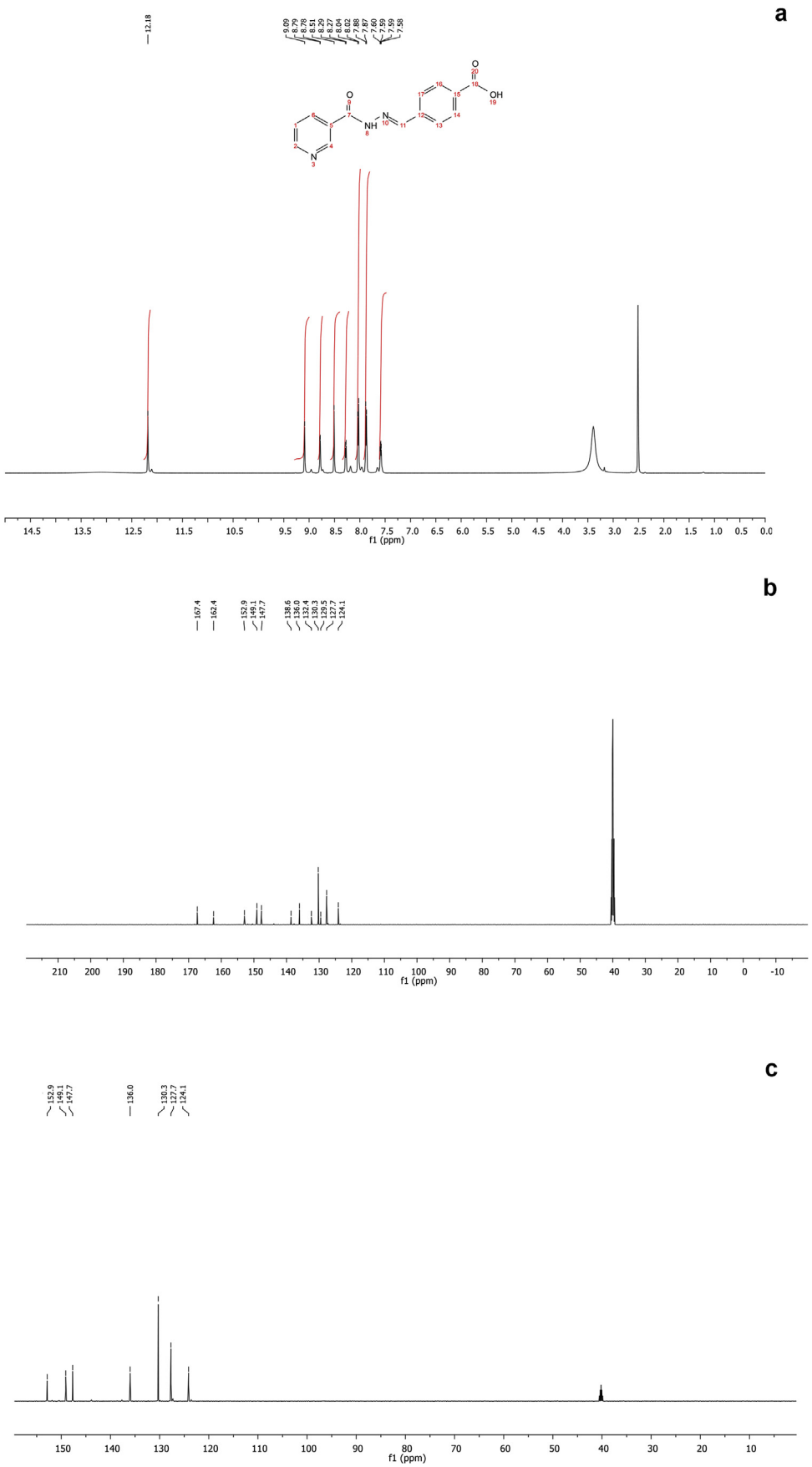

Fig. 2. (a) ^{1}H, (b) ^{13}C NMR (DMSO-d_6) and (c) DEPT spectra of the titled compound.

Table 1
The calculated and experimental ^{1}H and ^{13}C NMR isotropic chemical shifts of the titled compound (with respect to TMS, all values in ppm).

		6-311++G (d.p)		6-311 + G (2d.p)		6-311++G (2d.p)	
	Experiment.	B3LYP	HF	B3LYP	HF	B3LYP	HF
C14	167.4	171.8	167.3	171.2	166.9	171.8	167.0
C6	162.4	170.5	169.7	169.8	169.1	170.4	169.2
C7	152.9	156.8	156.2	155.9	155.1	156.4	155.2
C5	149.1	160.2	162.7	158.8	161.5	159.4	161.6
C1	147.7	152.7	155.9	151.6	154.6	152.3	154.7
C8	138.6	148.6	149.2	147.5	147.9	148.0	148.0
C3	136.0	143.3	150.7	141.8	149.4	142.4	149.5
C12	132.4	138.	140.9	137.0	139.3	137.5	139.4
C2	130.3	137.1	133.1	136.1	131.8	136.6	131.9
C10	129.5	137.0	140.0	135.7	138.4	136.2	138.5
C9	130.3	136.6	135.2	135.3	133.7	135.8	133.8
C11	127.4	135.8	134.2	134.8	133.2	135.4	133.3
C13	127.4	129.7	130.2	128.2	128.6	128.7	128.7
C4	124.1	129.6	126.2	127.8	124.5	128.4	124.6
H7	12.18	10.74	10.12	10.82	10.17	10.84	10.18
H1	9.09	9.02	9.19	9.11	9.24	9.14	9.24
H5	8.79	8.98	9.14	9.07	9.17	9.07	9.16
H2	8.51	8.77	7.75	8.89	7.82	8.90	7.82
H3	8.29	8.63	9.07	8.63	9.08	8.66	9.08
H13	7.88	8.57	8.72	8.56	8.67	8.57	8.66
H12	8.04	8.52	8.85	8.54	8.88	8.55	8.88
H10	8.02	8.36	8.61	8.41	8.64	8.43	8.63
H4	7.60	7.59	7.56	7.59	7.57	7.61	7.57
H9	7.87	7.56	7.77	7.61	7.82	7.63	7.83
H6	7.59	5.78	5.57	5.65	5.41	5.67	5.42

3.3. Conformational and structural analysis

In the result of conformation analysis, the plotted potential energy curves (PECs) of the molecule as a function of dihedral angles ϕ1 (C3—C2—C6—N2), ϕ2 (N3—C7—C8—C13) and ϕ3 (C10—C11—C14—O2) were given Fig. 6. During conformation analysis, all the geometrical parameters were concurrently relaxed but dihedral angles, ϕ1, ϕ2 and ϕ3 were varied in steps of 10° ranging from 0° to 360°. As shown in the Fig. 6, the global energy minimum on PECs was referred to as zero. The PECs obtained at B3LYP/6—31 G showed three minimum energy structures at the 0, 180 and 360° and two energy barrier at the 90 and 270°. Since the potential energy curves are symmetrical with respect to 180°, the barrier heights obtained for each dihedral angle have the same value. The barrier heights of ϕ1 (C3—C2—C6—N2), ϕ2 (N3—C7—C8—C13) and ϕ3 (C10—C11—C14—O2) dihedral angles were found to be 4.41, 8.09 and 9.02 kcal/mol, respectively.

The molecular structure of 4-[(pyridine-3-carbonyl)-hydrazonomethyl]-benzoic acid molecule was optimized using both HF and DFT/B3LYP methods using 6-311G++(d,p) basis set. The selected X-ray (experimental) [54] and the theoretical results of structure were given Table 3.

The carbon-carbon bond lengths were: C2—C6 1.5018 Å (B3LYP)/1.5004 Å (HF)/(4) Å 1.497 (4) Å (XRD) and C7—C8 1.4629 Å (B3LYP)/1.4766 Å (HF)/1.469 (4) Å (XRD). The carbon-nitrogen bond lengths were: C1—N1 1.3349 Å (B3LYP)/1.3198 Å (HF)/1.337 (4) Å (XRD), C5—N1 1.3357 Å (B3LYP)/1.3179 Å(HF)/1.336 (4) Å (XRD), C6—N2 1.3889 Å (B3LYP)/1.3697 Å(HF)/1.364 (4) Å (XRD) and C7=N3, 1.2805 Å (B3LYP)/1.2519 Å (HF)/1.281 (4) Å (XRD) The nitrogen - nitrogen bond lengths were: 1.3532 Å (B3LYP)/1.3512(HF)/1.389 (4) Å (XRD).

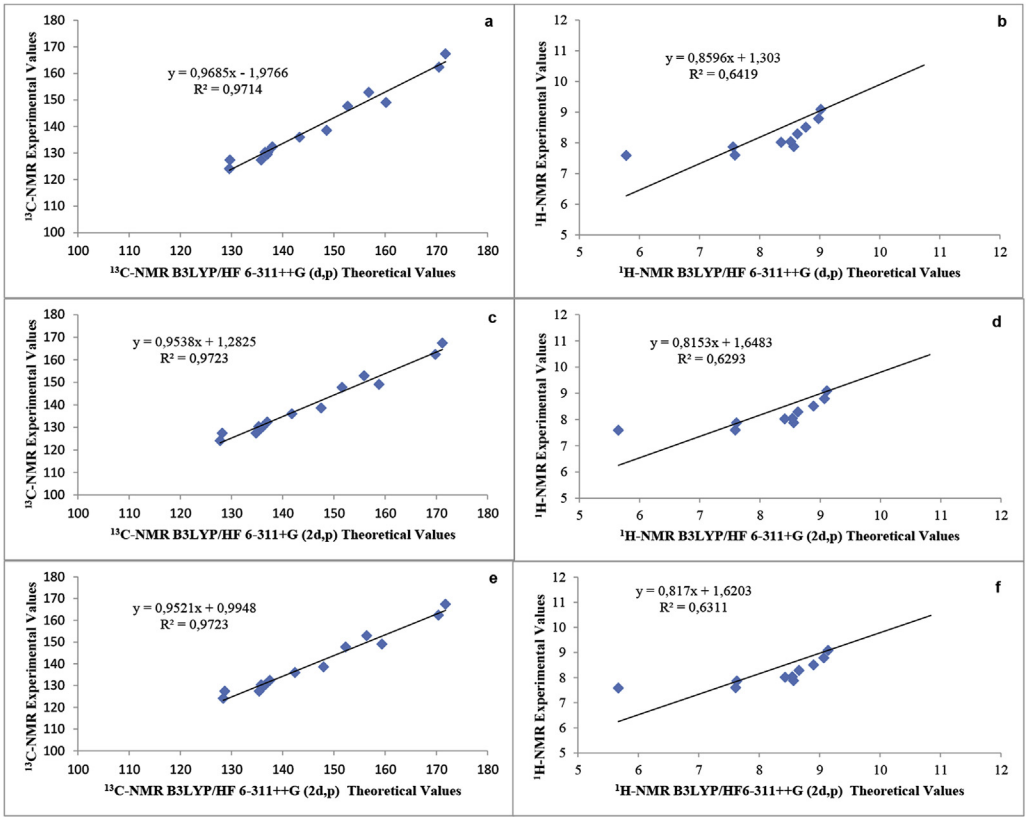

Fig. 3. The correlation graphics for 13C NMR B3LYP/HF 6—311++G (d,p) (a), 1H NMR B3LYP/HF 6—311++G (d,p) (b), 13C NMR B3LYP/HF 6-311 + G (2d,p) (c), 1H NMR B3LYP/HF 6-311 + G (2d,p) (d), 13C NMR B3LYP/HF 6—311++G (2d,p) (e) and 1H NMR B3LYP/HF 6—311++G (2d,p) (f) chemical shifts of the title compound.

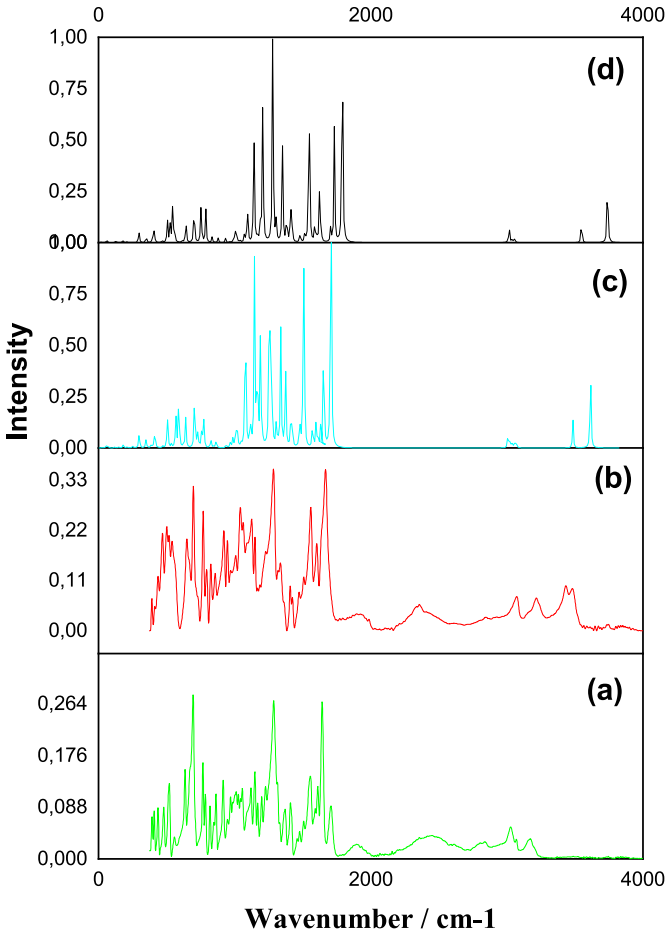

Fig. 4. Theoretical and experimental FT-IR Spectra of the titled compound (a) Theoretical FT-IR from HF/6−311++G (d,p) (with scalling factor); b) Theoretical FT-IR B3LTY/6−311++G (d,p) (with scalling factor); c) Experimental FT-IR spectra of 4-[(Pyridine-3-carbonyl)-hydrazonomethyl]-benzoic acid monohydrate; d) Experimental FT-IR spectra of 4-[(Pyridine-3-carbonyl)-hydrazonomethyl]-benzoic acid.

The carbon-oxygen bond lengths were: C6=O11.2117 Å (B3LYP)/1.1875 Å (HF)/1.225 (3) Å (XRD), C14 = O2 1.2089 Å (B3LYP)/1.1847 Å (HF) and C14−O3 1.3587 Å (B3LYP)/1.3288 Å (HF). The optimized parameters at both methods differ slightly from the XRD values and since the theoretical studies are performed on the gas phase rather than the solid state, very little deviation should be expected.

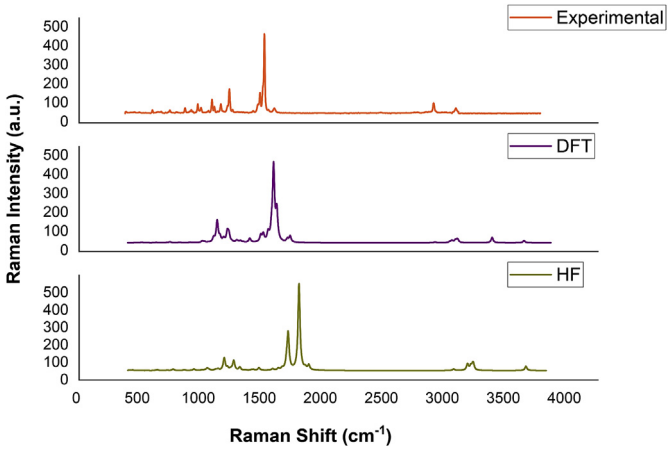

Fig. 5. FT-Raman Spectra of the title compund

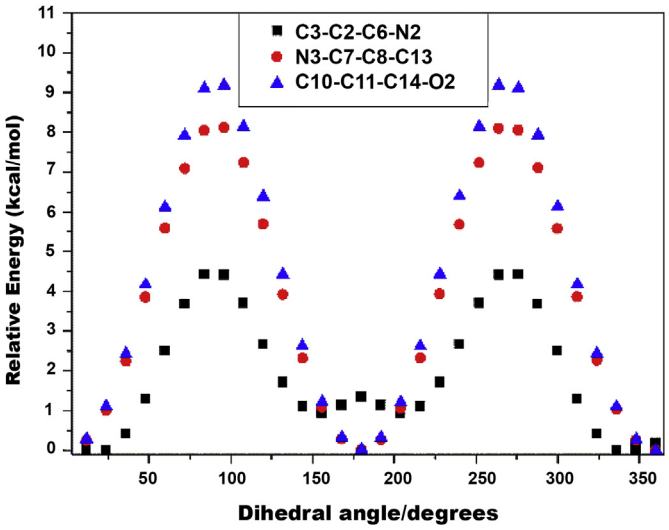

Fig. 6. Potential energy curves for the molecule with B3LYP/6-31G.

3.4. Electronic properties, HOMO-LUMO and MEP analysis

The UV−Vis spectra of the title compound were recorded in DMSO at room temperature. The experimental and theoretical electronic spectra of the title compound were given in Fig. S1. In the electronic spectra, n→π* and π→π* transitions are due to the presence of Q bands. The n→π* or π→π* transitions of the functional groups such as the benzene ring, pyridine ring, C=O, C=N were observed at 322 nm. This value was calculated to be 315 nm for the B3LYP/6-31G level [55].

The band gap, a fundamental physical feature of the molecules, can be described as minimum photon energy necessary to excite an electron from HOMO to LUMO. We determined the band gap of 4-[(pyridine-3-carbonyl)-hydrazonomethyl]-benzoic acid molecule obtained through the UV-3600 Plus UV-VIS-NIR Spectrophotometer with ISR-603 Integrating Sphere Attachment and carry out an ab-initio HF and DFT with B3LYP and LSDA level using 6−311++G (d.p) basis set. The iso-density plots of the HOMO and LUMO computed by the methods of B3LYP/6−311++G (d,p) of the studied compounds were shown in Fig. 7.

Also, the theoretically calculated electronic energy, dipole moment polarizability and hyperpolarizability values of the molecule and the HOMO and LUMO values obtained both theoretically and experimentally were given in Table 4.

The reflectance spectra obtained from UV−Vis−NIR Spectrophotometer were converted into equivalent absorption spectra by means of Kubelka-Munk function (Fig. 8). Kubelka-Munk method is based on following equation [56,57].

$$F(R) = (1 - R)^2 / 2R = \frac{K}{S}$$

Molecular Electrostatic Potential (MEP) gives important information about interactions ligand-substrate interactions and local reactivity of molecule. The MEP of the molecule computed at the DFT/B3LYP/6-311G++ (d, p) level of theory were given in Fig. 9.

The red and blue color regions on MEP surface represent nucleophilic and electrophilic site, respectively. With respect to the surface of MEP, the negative potential preferred site for electrophilic attack is formed around the oxygen atom of the carbonyl groups and nitrogen atom of imine group and pyridine ring. The

Table 3
The selected experimental and calculated sructure parameters of the molecule.

Bond Length (Å)	X-ray [54]	HF	B3LYP	Bond angle (°)	X-ray [54]	HF	B3LYP
C1–N1	1.337 (4)	1.3198	1.3349	C1–C2–C6	116.9 (3)	124.08	124.23
C2–C6	1.497 (4)	1.5004	1.5018	C3–C2–C6	119.3 (3)	118.16	118.01
C5–N1	1.336 (4)	1.3179	1.3357	C2–C6–O1	120.8 (3)	121.65	122.33
C6–N2	1.364 (4)	1.3697	1.3889	N2–C6–O1	122.9 (3)	123.71	123.39
C6–O1	1.225 (3)	1.1875	1.2117	C8–C7–N3	121.0 (3)	121.63	121.72
C7–C8	1.469 (4)	1.4766	1.4629	C7–C8–C9	120.0 (3)	118.95	119.10
C7–N3	1.281 (4)	1.2519	1.2805	C7–C8–C13	121.6 (3)	121.52	121.79
C11–C14	–	1.4882	1.4854	C6–N2–N3	119.0 (2)	120.13	120.94
C14–O2	–	1.1847	1.2089	C7–N3–N2	115.8 (3)	117.93	117.47
C14–O3	–	1.3288	1.3587	C2–C6–O1	120.8 (3)	121.65	122.33
N2–N3	1.389 (4)	1.3512	1.3532	O2–C14–O3	–	122.09	121.96
Dihedral angle (°)				Dihedral angle (°)			
C1–C2–C6–N2	−23.0 (5)	28.09	28.01	N3–C7–C8–C13	−1.1 (5)	−0.24	−0.29
C1–C2–C6–O1	154.3 (3)	−152.38	−152.71	C6–N2–N3–C7	178.8 (3)	−172.27	−175.92
C3–C2–C6–N2	163.7 (3)	−154.24	−154.68	C10–C11–C14–O3	–	−0.77	−0.01
C2–C6–N2–N3	168.6 (3)	−179.33	−177.56	C12–C11–C14–O2	–	−0.70	−0.01
N3–C7–C8–C9	−179.3 (3)	179.77	179.67	C12–C11–C14–O3	–	179.98	179.94

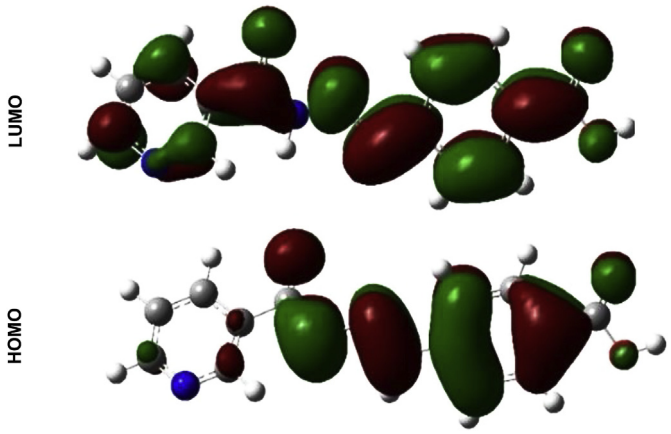

Fig. 7. Calculated HOMO-LUMO plots of the molecule with B3LYP/6−311++G (d,p).

positive potential is formed around the hydrogen atom of the carboxylic acid and attached to nitrogen atom (NH). The dipole moment value of title molecule has been found as 4.60 (B3LYP) and 5.09 Debye (HF). The hyperpolarizability values of the title molecule are 1299.49 (B3LYP) and 494.57 a. u (HF). The hyperpolarizability (β) values at the Gaussian 09 output are in atomic units (a.u) and these values converted into electrostatic unit (e.s.u) (for β: 1 a. u = 8.639 × 10 $^{-33}$ esu). Urea is one of the archetypal molecules used in the study of the NLO property of molecular systems. The calculated β value of urea by B3LYP/6−311++G (d,p) method is 0.3728 × 10−30 e. s.u. While comparing, β value of the title molecule is 30.11 times greater than that of urea. So, the of 4-[(pyridine-3-carbonyl)-hydrazonomethyl]-benzoic acid molecule is suitable for NLO device applications.

3.5. Thermal analysis

The obtained water molecule of 4-[(Pyridine-3-carbonyl)-hydrazonomethyl]-benzoic acid monohydrate removed in the temperature range of 50–200 °C that is accompanied by an endothermic peak on 160 °C (exp. 6.42%, calc. 6.27%). After this weight loss, the anhydrous compound is thermally stable up to 280 °C. The obtained title compound began to decompose at this temperature and the obtained compound was completely decomposed (exp. 97.66%) (Fig. 10).

4. Conclusion

A novel Schiff base derivative, 4-[(pyridine-3-carbonyl)-hydrazonomethyl]-benzoic acid was synthesized at a high yield by an original procedure from methyl nicotinate and hydrazine, followed by condensation with 4-carboxybenzaldehyde. It was characterized by ^{1}H, ^{13}C NMR, FT-IR, FT-Raman and UV–Vis spectroscopy. Although aroylhydrazones derived from nicotinic acid hydrazides are widely synthesized, studies comparing experimental data used for characterization of these compounds with those calculated theoretically are limited. Molecular geometry, vibrational wave numbers, frontier molecular orbital and non-linear optical (NLO) properties of the title compound were calculated using HF and B3LYP methods. The spectroscopic results obtained were compared with the results obtained using these methods. When experimental data from the ^{1}H and ^{13}C NMR spectroscopy were compared with theoretically calculated values, it was found that the results closest was obtained from the B3LYP/HF 6−311++G (d,p) method. In addition, LSD is considered to be the most appropriate calculation method for HOMO-LUMO values in this study. The nonlinear optical properties were calculated at DFT/B3LYP/6-311G++ (d, p) level of theory and it was found that the hyperpolarizability of the

Table 4
Electronic Energy, dipole moment (μ), polarizability (α) hyperpolarizability (β), E_{HOMO} and E_{LUMO} of the compound.

	DFT/6−311++G (d,p)	HF/6−311++G (d,p)	LSDA/6−311++G (d,p)	Experimental
Electronic Energy (a.u)	−930.292061803	−924.728961455		
μ (D)	4.60	5.09		
α (a.u)	230,74	192,67		
β (a.u)	1299,49	494,57		
E_{HOMO} (a.u)	−0.249004	−0.332458	−0,248427	
E_{LUMO} (a.u)	−0.096358	0.028088	−0,146743	
ΔEg (eV)	4.15	9,81	2,77	2.827

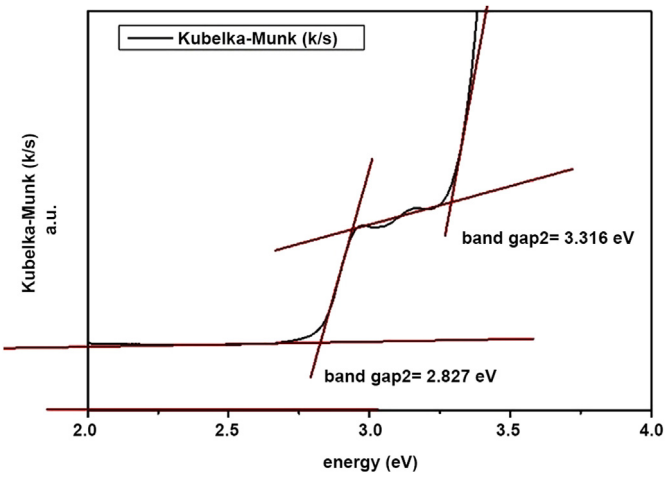

Fig. 8. Linear dependence of F(R) on the photon energy hυ corresponding to direct-allowed transitions.

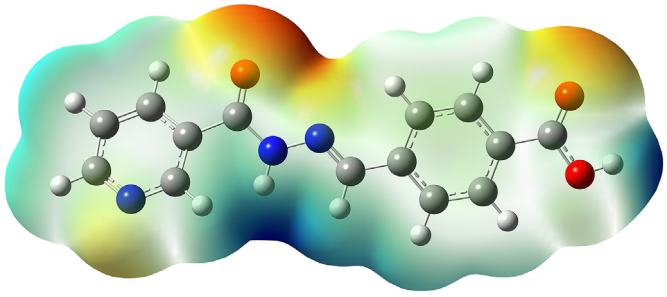

Fig. 9. MEP surfaces of the molecule.

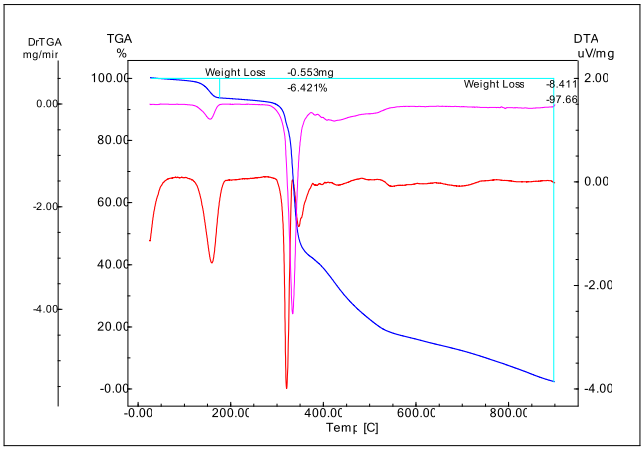

Fig. 10. TGA/DTA curves of 4-[(pyridine-3-carbonyl)-hydrazonomethyl]-benzoic acid monohydrate.

compound is 30.11 times greater than that of reference molecule (urea). According to these results, 4 - [(pyridine-3-carbonyl)-hydrazonometyl]-benzoic acid compound can be recommended for further studies as a suitable material for NLO device applications.

CRediT author statement

Füreya Elif Özbek: Writing-Reviewing and Editing and Evaluation of Results Güventürk Uğurlu.: Theoretical Calculations. Erbay Kalay: Synthesis and Evaluation of Results; Hacali Necefoğlu: Writing-Reviewing.

Declaration of competing interest

The authors declare that they have no known competing financial interests or personal relationships that could have appeared to influence the work reported in this paper.

Appendix A. Supplementary data

Supplementary data to this article can be found online at https://doi.org/10.1016/j.molstruc.2020.128247.

References

[1] R.R. Sharipova, I.Yu Strobykina, G.G. Mordovskoi, R.V. Chestnova, V.F. Mironov, V.E. Kataev, Antituberculosis activity of glycosides from Stevia rebaudiana and hybrid compounds of steviolbioside and pyridinecarboxylic acid hydrazides, Chem. Nat. Compd. 46 (2011) 902–905, https://doi.org/10.1007/s10600-011-9779-6.

[2] R. Sinha, U.V.S. Sara, R.L. Khosa, J. Stables, J. Jain, Nicotinic acid hydrazones: a novel anticonvulsant pharmacophore, Med. Chem. Res. 20 (2011) 1499–1504, https://doi.org/10.1007/s00044-010-9396-0.

[3] R. Narang, S.D. Sharma, B. Narasimhan, Evaluation of Anti-inflammatory activity of acid Hydrazide derivatives, Hygeia J. Drugs Med. 4 (2012) 15–20.

[4] M.B. Deshmukh, S.H. Patil, C.S. Shripanavar, Synthesis and insecticidal activity of some nicotinic acid derivatives, J. Chem. Pharmaceut. Res. 4 (2012) 326–332.

[5] R. Narang, B. Narasimhan, S. Sharma, D. Sriram, P. Yogeeswari, E. De Clercq, C. Pannecouque, J. Balzarini, Synthesis, antimycobacterial, antiviral, antimicrobial activities, and QSAR studies of nicotinic acid benzylidene hydrazide derivatives, Med. Chem. Res. 21 (2012) 1557–1576, https://doi.org/10.1007/s00044-011-9664-7.

[6] O. Kehinde, A. Joseph, S. Tolutope, A. Olanrewaju, A. Christiana, A. Kayode, M. Salih, N. Tadigoppula, Synthesis, characterization, theoretical treatment and antitubercular activity evaluation of (E)-N'- (2,5-dimethoxylbenzylidene) nicotinohydrazide and some of its transition metal complexes against Mycobacterium tuberculosis, H37Rv, Orient. J. Chem. 32 (2016) 413–427, https://doi.org/10.13005/ojc/320147.

[7] R. Sinha, U. Sara, R. Khosa, J. Stables, J. Jain, In silico validation and structure activity relationship study of a series of pyridine-3-carbohydrazide derivatives as potential anticonvulsants in generalized and partial seizures, Cent. Nerv. Syst. Agents Med. Chem. 13 (2013) 132–140, https://doi.org/10.2174/1871524911313020006.

[8] A. Moradi, L. Navidpour, M. Amini, H. Sadeghian, H. Shadnia, O. Firouzi, R. Miri, S.E.S. Ebrahimi, M. Abdollahi, M.H. Zahmatkesh, A. Shafiee, Design and synthesis of 2-phenoxynicotinic acid hydrazides as anti-inflammatory and analgesic agents, Archiv Der Pharmazie 343 (2010) 509–518, https://doi.org/10.1002/ardp.200900294.

[9] L. Navidpour, H. Shafaroodi, G. Saeedi-Motahar, A. Shafiee, Synthesis, anti-inflammatory and analgesic activities of arylidene-2-(3-chloroanilino)nicotinic acid hydrazides, Med. Chem. Res. 23 (2014) 2793–2802, https://doi.org/10.1007/s00044-013-0860-5.

[10] A. Budimir, T. Benković, V. Tomišić, A. Gojmerac Ivšić, N. Galić, Hydrolysis and extraction properties of aroylhydrazones derived from nicotinic acid hydrazide, J. Solut. Chem. 42 (2013) 1935–1948, https://doi.org/10.1007/s10953-013-0081-z.

[11] N. Galić, M. Rubčić, K. Magdić, M. Cindrić, V. Tomišić, Solution and solid-state studies of complexation of transition-metal cations and Al(III) by aroylhydrazones derived from nicotinic acid hydrazide, Inorg. Chim. Acta. 366 (2011) 98–104, https://doi.org/10.1016/j.ica.2010.10.017.

[12] X.-B. Li, J.-Y. Chen, E.-J. Wang, A highly selective and sensitive chemosensor for colorimetric and fluorescent detection of Al3+ and living cell imaging, Aust. J. Chem. 68 (2015) 156, https://doi.org/10.1071/CH14079.

[13] T. Benković, A. Kendel, J. Parlov-Vuković, D. Kontrec, V. Chiş, S. Miljanić, N. Galić, Aromatic hydrazones derived from nicotinic acid hydrazide as fluorimetric pH sensing molecules: structural analysis by computational and spectroscopic methods in solid phase and in solution, Spectrochim. Acta Mol. Biomol. Spectrosc. 190 (2018) 259–267, https://doi.org/10.1016/j.saa.2017.09.038.

[14] P.A.L. Anawe, C.U. Obi, S.S. Mehdi, K.O. Ogunniran, B.I. Ita, C.O. Ehi-Eromosele, Experimental and theoretical studies of (E)-N′-1-(4-propylbenzylidene)nicotinohydrazide as corrosion inhibitor of mild steel in 1 M HCl, Protect. Met. Phys. Chem. Surface 51 (2015) 458–466, https://doi.org/10.1134/S2070205115030041.

[15] N. Galić, B. Perić, B. Kojić-Prodić, Z. Cimerman, Structural and spectroscopic characteristics of aroylhydrazones derived from nicotinic acid hydrazide, J. Mol. Struct. 559 (2001) 187–194, https://doi.org/10.1016/S0022-2860(00)

00703-1.
[16] N. Galić, I. Brođanac, D. Kontrec, S. Miljanić, Structural investigations of aroylhydrazones derived from nicotinic acid hydrazide in solid state and in solution, Spectrochim. Acta Mol. Biomol. Spectrosc. 107 (2013) 263–270, https://doi.org/10.1016/j.saa.2013.01.028.
[17] D. Stražić, T. Benković, D. Gembarovski, D. Kontrec, N. Galić, Comprehensive ESI-MS and MS/MS analysis of aromatic hydrazones derived from nicotinic acid hydrazide, Int. J. Mass Spectrom. 371 (2014) 54–64, https://doi.org/10.1016/j.ijms.2014.07.036.
[18] T. Benković, D. Kontrec, V. Tomišić, A. Budimir, N. Galić, Acid–base properties and kinetics of hydrolysis of aroylhydrazones derived from nicotinic acid hydrazide, J. Solut. Chem. 45 (2016) 1227–1245, https://doi.org/10.1007/s10953-016-0504-8.
[19] A. Manimekalai, N. Saradhadevi, A. Thiruvalluvar, Molecular structures, spectral and computational studies on nicotinohydrazides, Spectrochim. Acta Mol. Biomol. Spectrosc. 77 (2010) 687–695, https://doi.org/10.1016/j.saa.2010.06.031.
[20] W.-X. Xu, Y.-M. Yuan, W.-H. Li, Syntheses, crystal structures, and catalysis by polymeric dioxomolybdenum(VI) complexes with similar (iso)nicotinohydrazones, J. Coord. Chem. 66 (2013) 2726–2735, https://doi.org/10.1080/00958972.2013.816416.
[21] A.-M. Li, Vanadium(V) complexes with hydrazone and benzohydroxamate ligands: synthesis, structures and catalytic epoxidation, J. Coord. Chem. 67 (2014) 2076–2085, https://doi.org/10.1080/00958972.2014.931577.
[22] J.-C. Castillo, A. Tigreros, J. Portilla, 3-Formylpyrazolo[1,5- *a*]pyrimidines as key intermediates for the preparation of functional fluorophores, J. Org. Chem. 83 (2018) 10887–10897, https://doi.org/10.1021/acs.joc.8b01571.
[23] S. Shen, H. Chen, T. Zhu, X. Ma, J. Xu, W. Zhu, R. Chen, J. Xie, T. Ma, L. Jia, Y. Wang, C. Peng, Synthesis, characterization and anticancer activities of transition metal complexes with a nicotinohydrazone ligand, Oncology Letters 13 (2017) 3169–3176, https://doi.org/10.3892/ol.2017.5857.
[24] K.O. Ogunniran, M.A. Mesubi, K.V.S.N. Raju, T. Narender, Structural and in vitro anti-tubercular activity study of (E)-N'-(2,6-dihydroxybenzylidene)nicotinohydrazide and some transition metal complexes, J. Iran. Chem. Soc. 12 (2015) 815–829, https://doi.org/10.1007/s13738-014-0544-1.
[25] O. Kehinde Olurotimi, A. Joseph Adeyemi, B. Omolara Agbeke, O. Olajumoke, S. Tolutope Oluwasegun, E. Godfery Sunday, Structural and biological activity study of (E)-N'- (5-chloro-2-Hydroxybenzylidene)Nicotinohydrazide) [H2L] and some of its divalent metal complexes, Orient. J. Chem. 33 (2017) 1623–1635, https://doi.org/10.13005/ojc/330405.
[26] A. Trzesowska-Kruszynska, On construction of lead coordination polymers derived from *N* ′-(2-hydroxybenzylidene)nicotinohydrazide via covalent and non-covalent interactions, J. Coord. Chem. 67 (2014) 120–135, https://doi.org/10.1080/00958972.2013.876494.
[27] G. Mahmoudi, D.A. Safin, M.P. Mitoraj, M. Amini, M. Kubicki, T. Doert, F. Locherer, M. Fleck, Anion-driven tetrel bond-induced engineering of lead(ii) architectures with N′-(1-(2-pyridyl)ethylidene)nicotinohydrazide: experimental and theoretical findings, Inorganic Chemistry Frontiers 4 (2017) 171–182, https://doi.org/10.1039/C6QI00477F.
[28] Y.-Q. Su, C. Li, P. Wang, *E*)- *N* ′-(3,5-Dibromo-2-hydroxybenzylidene)nicotinohydrazide, Acta Crystallographica Section E Structure Reports Online 66 (2010), https://doi.org/10.1107/S1600536810006276 o670–o670.
[29] P. Wang, C. Li, Y.-Q. Su, *N* ′-(2-Methoxybenzylidene)nicotinohydrazide, Acta Crystallographica Section E Structure Reports Online 66 (2010), https://doi.org/10.1107/S1600536810003831 o542–o542.
[30] X.-W. Zhu, Y.-J. Zhang, C.-X. Zhang, H.-Y. Qian, Crystal structure of (E)-N'-(4-(diethylamino)-2-hydroxybenzylidene) nicotinohydrazide—water (1:1), C17H20N4O2 · H2O, Z. Kristallogr. N. Cryst. Struct. 226 (2011) 375–376, https://doi.org/10.1524/ncrs.2011.0168.
[31] S.-S. Sun, S.-Y. Liu, T.-T. Zheng, X.-L. Wang, *E*)- *N* ′-(2-Hydroxy-3,5-diiodobenzylidene)nicotinohydrazide acetonitrile monosolvate, Acta Crystallographica Section E Structure Reports Online 67 (2011), https://doi.org/10.1107/S1600536811020770 o1624–o1624.
[32] M. Prabhu, K. Parthipan, A. Ramu, G. Chakkaravarthi, G. Rajagopal, *E*)- *N* ′-(3-Bromo-5-chloro-2-hydroxybenzylidene)nicotinohydrazide, Acta Crystallographica Section E Structure Reports Online 67 (2011), https://doi.org/10.1107/S1600536811038268 o2716–o2716.
[33] S. Sravya, S. Sruthy, N. Aiswarya, M. Sithambaresan, M.R.P. Kurup, Crystal structure of (*E*)- *N* ′-(5-bromo-2-hydroxybenzylidene)nicotinohydrazide monohydrate, Acta Crystallographica Section E Crystallographic Communications 71 (2015) 734–736, https://doi.org/10.1107/S2056989015009627.
[34] N. Dege, N. Şenyüz, H. Batı, N. Günay, D. Avcı, Ö. Tamer, Y. Atalay, The synthesis, characterization and theoretical study on nicotinic acid [1-(2,3-dihydroxyphenyl)methylidene]hydrazide, Spectrochimica Acta Part A: Molecular and Biomolecular Spectroscopy 120 (2014) 323–331, https://doi.org/10.1016/j.saa.2013.10.030.
[35] T. Benković, A. Kenđel, J. Parlov-Vuković, D. Kontrec, V. Chiş, S. Miljanić, N. Galić, Multiple dynamics of aroylhydrazone induced by mutual effect of solvent and light - spectroscopic and computational study, J. Mol. Liq. 255 (2018) 18–25, https://doi.org/10.1016/j.molliq.2018.01.158.
[36] R. Dennington, T. Keith, J. Millam, Semichem inc., GaussView, version 5, Shawnee Mission KS (2009) n.d.
[37] M. Frisch, G. Trucks, H. Schlegel, G. Scuseria, M. Robb, J. Cheeseman, G. Scalmani, V. Barone, B. Mennucci, G. Petersson, H. Nakatsuji, M. Caricato, X. Li, H. Hratchian, A. Izmaylov, J. Bloino, G. Zheng, J. Sonnenberg, M. Hada, M. Ehara, K. Toyota, R. Fukuda, J. Hasegawa, M. Ishida, T. Nakajima, Y. Honda, O. Kitao, H. Nakai, T. Vreven, J. Montgomery, J. Peralta, F. Ogliaro, M. Bearpark, J. Heyd, E. Brothers, K. Kudin, V. Staroverov, R. Kobayashi, J. Normand, K. Raghavachari, A. Rendell, J. Burant, S. Iyengar, J. Tomasi, M. Cossi, N. Rega, J. Millam, M. Klene, J. Knox, J. Cross, V. Bakken, C. Adamo, J. Jaramillo, R. Gomperts, R. Stratmann, O. Yazyev, A. Austin, R. Cammi, C. Pomelli, J. Ochterski, R. Martin, K. Morokuma, V. Zakrzewski, G. Voth, P. Salvador, J. Dannenberg, S. Dapprich, A. Daniels, J. Foresman Farkas, J. Ortiz, J. Cioslowski, D. Fox, Gaussian 09, Revision B.01, Gaussian 09, Revision B.01, Gaussian, Inc., Wallingford CT, 2009.
[38] Chr Møller, M.S. Plesset, Note on an approximation treatment for many-electron systems, Phys. Rev. 46 (1934) 618–622, https://doi.org/10.1103/PhysRev.46.618.
[39] A.D. Becke, Density-functional exchange-energy approximation with correct asymptotic behavior, Phys. Rev. 38 (1988) 3098–3100, https://doi.org/10.1103/PhysRevA.38.3098.
[40] C. Lee, W. Yang, R.G. Parr, Development of the Colle-Salvetti correlation-energy formula into a functional of the electron density, Phys. Rev. B 37 (1988) 785–789, https://doi.org/10.1103/PhysRevB.37.785.
[41] A.D. Becke, Density-functional thermochemistry. III. The role of exact exchange, J. Chem. Phys. 98 (1993) 5648–5652, https://doi.org/10.1063/1.464913.
[42] M.M. Francl, W.J. Pietro, W.J. Hehre, J.S. Binkley, M.S. Gordon, D.J. DeFrees, J.A. Pople, Self-consistent molecular orbital methods. XXIII. A polarization-type basis set for second-row elements, J. Chem. Phys. 77 (1982) 3654–3665, https://doi.org/10.1063/1.444267.
[43] V.A. Rassolov, M.A. Ratner, J.A. Pople, P.C. Redfern, L.A. Curtiss, 6-31G* basis set for third-row atoms, J. Comput. Chem. 22 (2001) 976–984, https://doi.org/10.1002/jcc.1058.
[44] L.G. Wade, Organic Chemistry, 6. ed, Pearson Prentice Hall, Upper Saddle River, NJ, 2006.
[45] A.U. Rani, N. Sundaraganesan, M. Kurt, M. Cinar, M. Karabacak, FT-IR, FT-Raman, NMR spectra and DFT calculations on 4-chloro-N-methylaniline, Spectrochim. Acta Mol. Biomol. Spectrosc. 75 (2010) 1523–1529, https://doi.org/10.1016/j.saa.2010.02.010.
[46] N. Subramanian, N. Sundaraganesan, J. Jayabharathi, Molecular structure, spectroscopic (FT-IR, FT-Raman, NMR, UV) studies and first-order molecular hyperpolarizabilities of 1,2-bis(3-methoxy-4-hydroxybenzylidene)hydrazine by density functional method, Spectrochim. Acta Mol. Biomol. Spectrosc. 76 (2010) 259–269, https://doi.org/10.1016/j.saa.2010.03.033.
[47] H. Yüksek, O. Gürsoy, I. Cakmak, M. Alkan, Synthesis and GIAO NMR calculations for some new 4,5-dihydro-1H-1,2,4-triazol-5-one derivatives: comparison of theoretical and experimental1H and13C chemical shifts, Magn. Reson. Chem. 43 (2005) 585–587, https://doi.org/10.1002/mrc.1591.
[48] M. Beytur, O. Akyildirim, S. Manap, H. Yüksek, Synthesis, molecular structure, spectral and electronic properties of 2-(3-Hydroxy-4-methoxybenzylideneamino)-5-mercapto-1,3,4- thiadiazole compound, Journal of the Institute of Science and Technology 8 (2018) 229–238, https://doi.org/10.21597/jist.426556.
[49] M. Beytur, Z. Turhan Irak, S. Manap, H. Yüksek, Synthesis, characterization and theoretical determination of corrosion inhibitor activities of some new 4,5-dihydro-1H-1,2,4-Triazol-5-one derivatives, Heliyon 5 (2019), e01809, https://doi.org/10.1016/j.heliyon.2019.e01809.
[50] H. Tereci, İ. Askeroğlu, N. Akdemir, İ. Uçar, O. Büyükgüngör, Combined experimental and theoretical approaches to the molecular structure of 4-(1-formylnaphthalen-2-yloxy)phthalonitrile, Spectrochim. Acta Mol. Biomol. Spectrosc. 96 (2012) 569–577, https://doi.org/10.1016/j.saa.2012.07.005.
[51] H. Pir, N. Günay, Ö. Tamer, D. Avcı, Y. Atalay, Theoretical investigation of 5-(2-Acetoxyethyl)-6-methylpyrimidin-2,4-dione: conformational study, NBO and NLO analysis, molecular structure and NMR spectra, Spectrochim. Acta Mol. Biomol. Spectrosc. 112 (2013) 331–342, https://doi.org/10.1016/j.saa.2013.04.063.
[52] D.L. Pavia, G.M. Lampman, G.S. Kriz, Introduction to Spectroscopy: a Guide for Students of Organic Chemistry, 3. ed, Brooks/Cole, South Melbourne, 2001.
[53] R.M. Silverstein, F.X. Webster, D.J. Kiemle, D.L. Bryce (Eds.), Spectrometric Identification of Organic Compounds, 8. ed, Wiley, Hoboken, NJ, 2015.
[54] M.S. Alam, D.-U. Lee, Quantum-chemical studies to approach the antioxidant mechanism of nonphenolic hydrazone Schiff base analogs: synthesis, molecular structure, hirshfeld and density functional theory analyses, Bull. Kor. Chem. Soc. 36 (2015) 682–691, https://doi.org/10.1002/bkcs.10132.
[55] H. Suzuki, Electronic Absorption Spectra and Geometry of Organic Molecules an Application of Molecular Orbital Theory, Elsevier Science, Burlington, 2012.
[56] M.L. Myrick, M.N. Simcock, M. Baranowski, H. Brooke, S.L. Morgan, J.N. McCutcheon, The kubelka-munk diffuse reflectance formula revisited, Appl. Spectrosc. Rev. 46 (2011) 140–165, https://doi.org/10.1080/05704928.2010.537004.
[57] L.A. Greenawald, J.L. Snyder, N.L. Fry, M.J. Sailor, G.R. Boss, H.O. Finklea, S. Bell, Development of a cobinamide-based end-of-service-life indicator for detection of hydrogen cyanide gas, Sensor. Actuator. B Chem. 221 (2015) 379–385, https://doi.org/10.1016/j.snb.2015.06.085.